ARTICLE   OPEN

Anthropogenic warming disrupts intraseasonal monsoon stages and brings dry-get-wetter climate in future East Asia

Lun Dai[1], Tat Fan Cheng [1] and Mengqian Lu [1]✉

East Asia will face a skewed monsoon cycle with soaring flood, drought, and weather whiplash risks in a warming climate. In our objective eight-intraseasonal-monsoon-stage framework, we uncover a 'dry-get-wetter' paradigm in East Asia, contesting the fallen 'rich-get-richer' common belief. On timing, the Mid-summer and Fall periods are stretching at the expense of three delayed, shortened, and weakened winter stages, especially near the end of the twenty-first century. On threats, entire East Asia will experience up to 14–20 more heavy precipitation days during the rainy Spring to Mid-summer stages. Specifically, the Yangtze basin will suffer from an earlier pluvial period with escalating flood risks. Moreover, societal security and ecosystem resilience in the Huai-Yellow basin, South Japan, and the Korean Peninsula will be challenged by more frequent weather whiplash. Under the monsoon-stage framework, a complete moisture budget decomposition sheds light on the causes of a slower precipitation scaling and the 'dry-get-wetter' paradigm.

npj Climate and Atmospheric Science (2022)5:11 ; https://doi.org/10.1038/s41612-022-00235-9

INTRODUCTION

The East Asian monsoon (EAM) is a subtropical monsoon system north of 20˚N featuring a seasonal reversal of winds and a contrast between rainy and dry seasons[1,2]. On a large scale, it is fundamentally driven by seasonally-varying solar radiations, shaped by the land-sea thermal contrast and upper-level westerly jets due to Tibetan Plateau forcing[1,3–6]. In recent decades, growing concerns over future changes of the EAM in a warming climate are warranted given its profound influence on the livelihoods of more than 1.5 billion people, plus the large uncertainties presented by climate model projections of monsoon precipitation, circulations, and seasonality[7–11].

Response of the EAM's seasonality to future radiative forcing has been analyzed commonly using precipitation-based monsoon indices[10–13]. Multiple lines of evidence suggested that the future wet season in East Asia seemed stretched with a remarkably delayed retreat[10–14] and at the expense of the dry duration[15]. While most studies focused on seasonal changes in the future[10–14], there remains a dearth of research on the future evolution of intraseasonal monsoon circulations and rainband featured by the EAM system[1,16], which are more relevant to climate- and weather-related activities. For this reason, we follow a recently developed circulation-based clustering approach to derive the EAM annual cycle[17]. The monsoon cycle consists of eight intraseasonal monsoon stages, among which the Early-, Mid-, and Late-winter stages manifest in anticyclonic circulations and widespread dry-and-cold air masses in East Asia, which are most dominant in the Mid-winter. Following the Late-winter, low-level southwesterlies become prominent in the south during the Spring and a quasi-stationary rain belt is then formed in South China during the Pre-Meiyu. The summertime southwesterlies peak in the ensuing Meiyu season, alongside the strongest monsoon rain belts lingering over the Yangtze basin and South Japan. The Mid-summer sees a continent-wide weakening of summer monsoons followed by the rise of anticyclonic circulations in the Fall, which completes the annual monsoon cycle. A multi-model weighting scheme is proposed to integrate the climate model outputs based

on their competence in reproducing the observed EAM annual cycle (see 'Methods'). Using such a framework, projected changes in the monsoon onset, retreat, and precipitation will facilitate more specific and comprehensive policies in optimizing irrigation schemes, sowing and harvesting, reservoir management, and climate adaptations in each intraseasonal stage[18].

Another moot point lies in the causes of the climate sensitivity of monsoon precipitation to greenhouse warming[9,19–24]. While water vapors in the atmosphere largely follow the Clausius-Clapeyron (C-C) rate (i.e., ~7% K^{-1})[12,19,21,25–27], future precipitation change is likely to scale at a much slower rate than that, suggesting additional processes at work to offset the moistening of the atmosphere. Scientists certified that the thermodynamic effect could be counteracted by an overall slowdown of atmospheric circulations[9,19,20,24,28,29], plausibly due to an increased atmospheric static stability in both lower and upper troposphere[14,30,31]. Paradoxical as it may seem, some studies indicated that East Asia might expect both enhanced precipitation and strengthened monsoon circulation manifested by an increase in lower-level and upper-level winds[32] as well as ascending motions[21]. Apparently, further investigation on the attributions to the future precipitation change in East Asia is much needed. Seeing that the monsoon climate in East Asia features pronounced variabilities within seasons, we show that the governing physical processes could be markedly different in well-defined intraseasonal stages, offering additional insights into the causes of precipitation changes under anthropogenic warming, and benefiting climate model evaluation and projection.

Here we propose a framework to assess the future monsoon cycle that fills the knowledge gap in the projected changes of intraseasonal monsoon stages in East Asia under two emission scenarios, the mitigated (i.e., the Representative Concentration Pathway 4.5 (RCP4.5)) and business-as-usual (RCP8.5) scenarios, based on the well-archived Coupled Model Intercomparison Project Phase 5 (CMIP5) model outputs (see 'Data' section). Under this framework, we discover a skewed monsoon cycle and diverse responses of the monsoon precipitation, hydrological extremes

[1]Department of Civil and Environmental Engineering, The Hong Kong University of Science and Technology, Clear Water Bay, Hong Kong, China. ✉email: mengqian.lu@ust.hk

and compound events in six East Asian land regions. Through the lens of a complete moisture budget decomposition, the physical processes that govern the future precipitation change in various monsoon stages are pinpointed. Lastly, we discuss the sensitivity of the monsoon precipitation field to greenhouse warming and the unexpectedly 'dry-get-wetter' paradigm in East Asia.

RESULTS

A skewed EAM annual cycle

Knowledge of the projected changes in the intraseasonal monsoon stages is vital to agrarian activity, freshwater security, and disaster adaptations in East Asia. Interestingly, timings and lengths of the Mid-summer, Fall, and the winter stages are highly susceptible to radiative forcings, while the temporal features of the rainy stages will barely change (Fig. 1 and Supplementary Fig. 1). Under the high-end scenario, we expect a significantly late retreat of both the Mid-summer and the Fall over the course of the 21st century (Fig. 1b). The late retreat contributes to prolonged Mid-summer (4.4–6.3 days longer) and Fall (~2.4 days longer) in the mid- (2041–2070) and long-term (2071–2100) future (Fig. 1c). However, changes in their onset dates appear less coherent, exemplified by an earlier onset of the Mid-summer by 2.8 days but a delayed Fall onset by 3.8 days in the future (Fig. 1a). These changes collectively explain a larger growth (+15.3%) in Mid-summer than Fall (+6.4%) in terms of the stage length (Fig. 1c), coinciding well with the lengthened rainy season as reported previously[10,12–14].

As surface warming can be amplified via the positive snow/ice-albedo feedback[33], it is not surprising to expect significant changes in the winter stages. Specifically, all the three winter stages will consistently delay their commencements by 3.6–6.5 days on average in the late-21st century (Fig. 1a), while the Early- and Mid-winter will retreat later by 4.3 and 5.8 days, respectively (Fig. 1b). Collectively, the Early- and Mid-winter will delay significantly without much variation in the stage days, whereas the Late-winter will shorten evidently by 2.6–4.6 days in the mid- and long-term future (Fig. 1c). Notably, the Pre-Meiyu, and the Early- and Late-winter exhibit a mild but significant reduction in their stage persistence (see 'Methods'), suggesting more intermittent Pre-Meiyu and winter monsoon seasons than before (Fig. 1d).

Taken together, the monsoon cycle in East Asia is likely to skew under a warming climate, as manifested in a markedly shortened transition from the cold to the warm season but a leisurely lengthened transition in reverse (i.e., the Fall stage). This finding locates one of the systematic changes in the future EAM cycle regardless of the high-emission or mitigated scenario (Supplementary Fig. 1).

Soaring risks of weather extremes and whiplash

Previous studies revealed a model unanimity on intensified precipitation extremes[12] and prolonged dry spells in East Asia under anthropogenic warming[13]. Here we revisit the projected likelihood of dry and heavy precipitation days (see 'Methods' for definitions) in six East Asian land regions throughout the annual cycle of monsoon. The projected changes in hydrological extremes and weather swings, as shown next, can be markedly different across regions and monsoon stages.

In general, East Asia will face soaring flood risks during the rainy season over the 21st century under both scenarios. We estimate on average 14–20 more heavy precipitation days in all land regions from the Spring to the Mid-summer in the long-term future (Fig. 2a). Remarkably, the Mid-summer alone contributes 6.4–12 more heavy precipitation days to the rainy season in all regions except the mid-lower Yangtze River basin (MLYRB), leading to a 50–200% increase in the likelihood of downpour for

the stage. Such a heightened flood risk, to some extent, results from a lengthened Mid-summer under a warmed climate (see 'A skewed EAM annual cycle' section).

Floods could also catch people off guard with early arrivals under greenhouse warming. The pluvial period in the MLYRB is likely to advance, given 6.6 more heavy precipitation days in the Spring during the long-term future of the high-emission scenario (Fig. 2a(2)). The advanced rainy season is attributable to a northward shift of future springtime rainbands since the mid-21st century (Fig. 3a(1)–(4)). Worse still, the enhanced spring rain in the MLYRB will, conceivably, compound with the thawing of snow and potential outbursts from ice-dammed glacial lakes in the upstream Tibetan Plateau[34], causing more devastating and earlier floods in the basin than ever before. Likewise, concerning regions in the north (i.e., the Huai-Yellow River basin (HYRB), North China and the Korean Peninsula), Meiyu rain belts extend significantly to the north (Fig. 3c(1)–(4)). On the bright side, an earlier and lengthened rainy season for northern regions might be conducive to local agriculture. However, flood control measures will have to be exercised earlier than their historical flood season (i.e., the Mid-summer)[1,17,35] to prepare for advanced flooding under a warming climate.

It may be unexpected that stronger northeasterly monsoons during the Fall and the Early-winter are tied to greenhouse warming (Fig. 3e, f(3), (4)), giving rise to 1–5 more dry days in all regions near the end of the century (Fig. 2b). As such, East Asia will lean towards water scarcity, heatwaves and bushfires when transitioning to the cold season under a warmer climate. While suppressed precipitation over the oceans, South Japan and South China will propagate throughout the winter season, regions in the north (i.e., the HYRB, North China, and the Korean Peninsula) may expect more snowfall or cold rains given 3–6 fewer dry days in the Mid- or Late-winter (Fig. 2b (3), (4) and (6)). This result reveals a dichotomy between a 'dry-get-drier' and a 'dry-get-wetter' winter climate in different parts of East Asia.

With the projected rise in both dry and wet extremes, we pay special attention to the weather whiplash, which denotes an abrupt shift between downpours and droughts within a short period of time (see 'Methods'). Such a compound extreme could trigger more ruinous impacts on the societies and ecosystems than individual weather extremes, yet it was rarely examined in climate change studies. In the long-term future of the high-emission scenario, almost entire East Asia will experience more frequent weather whiplash than before throughout the year (Fig. 2c). For the HYRB, South Japan and the Korean Peninsula that are historically prone to weather whiplash[36,37], they are projected to suffer more weather swings during the Spring, Pre-Meiyu, Fall and the Early-winter.

It is worth mentioning that weather extremes under the high-end scenario tend to increase monotonically from near-term to long-term future (Supplementary Fig. 2), while the mitigated scenario shares similar trends in hydrological risks at a smaller magnitude (Supplementary Figs. 3 and 4). This signifies a big difference in the future hydrological risks contingent on our efforts to reduce carbon emissions.

Attributions of changing precipitation under global warming

Inasmuch as the prominent changes in hydrological risks during future monsoon stages, we revisit a fundamental question about the mechanisms that govern the changing precipitation in the framework of the monsoon cycle. Here we gain insights into the contributions of various physical processes from a complete moisture budget decomposition (see 'Methods'). They include the moisture-driven thermodynamic (δTH_h and δTH_v), dynamic (δDY), vertical motion (δVM) and the transient eddy (δTE) effects in $\delta(P-E)$ during the long-term future under the RCP8.5 scenario, when changes are most salient. Note that the nonlinear and water
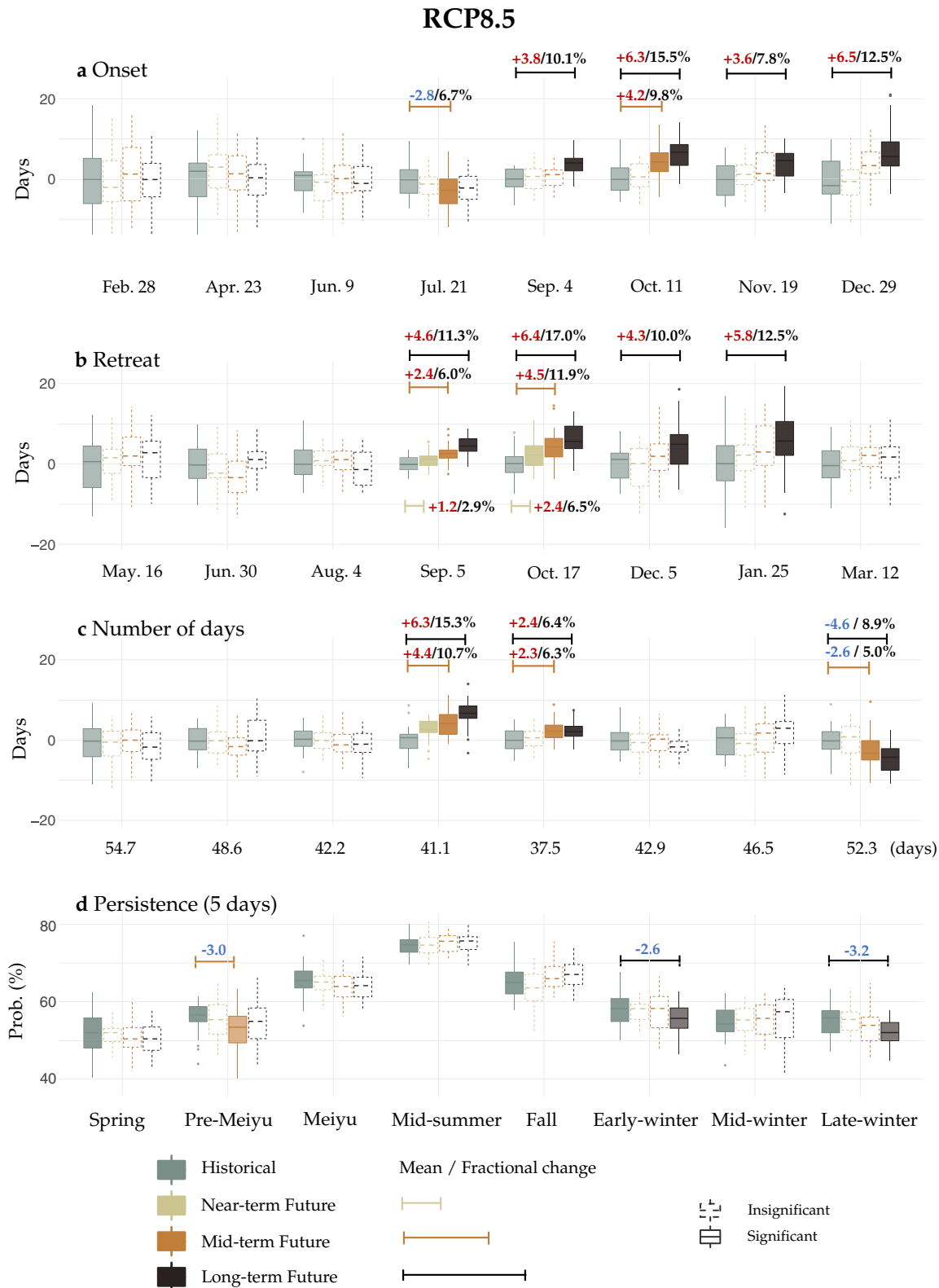
RCP8.5

Fig. 1 Projected changes in the temporal characteristics of monsoon stages. Boxplots showing interannual variations of **a** the onset date, **b** retreat date, **c** number of days and **d** the 5-day persistence (see 'Methods' for their definitions) of each monsoon stage in the near-term (2011–2040), mid-term (2041–2070), long-term (2071–2100) future compared with historical period (1971–2000) under the RCP8.5 scenario. The historical means of each monsoon stage's onset date, retreat date and the number of days are provided in the x-axis of the **a**, **b**, and **c**, respectively. A solid boxplot indicates a statistically significant difference between the projected and historical mean at the 0.05 level (Student's t-test) and is labeled with the corresponding values and fractional changes. The boxplots illustrate the median, the interquartile range, the upper (lower) whisker extending from the hinge to the largest (smallest) value no further than 1.5× interquartile range, and outliers as individual points.
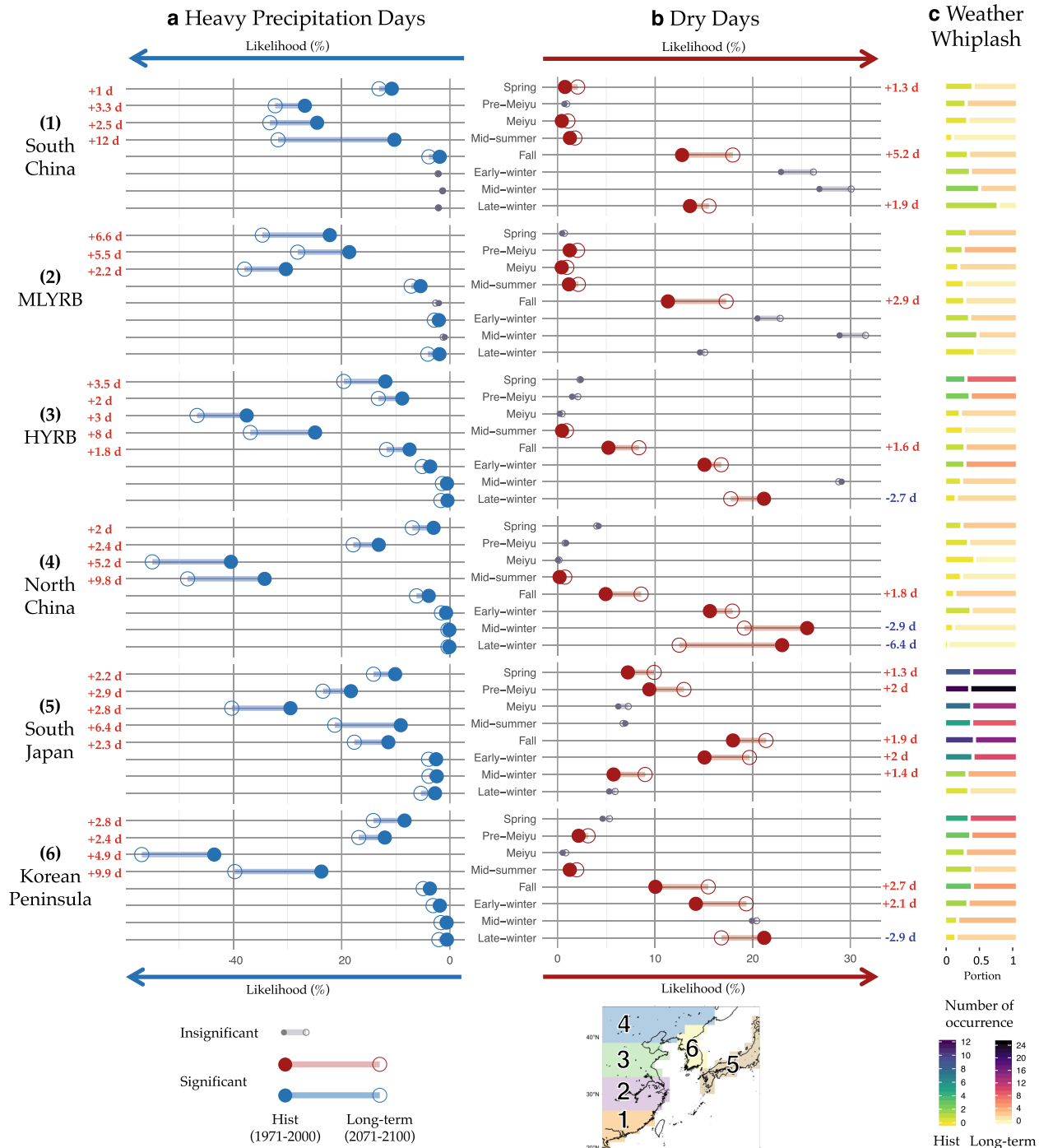
Fig. 2 Projected changes in hydrological risks over six East Asian land regions. 30-year averaged multi-model weighted probability of occurrence (or likelihood) (unit: %) of **a** heavy precipitation days and **b** dry days during each monsoon stage (see 'Methods') under the RCP8.5 scenario. Solid and hollow circles indicate the mean values for the historical period (1971–2000) and the long-term future (2071–2100), respectively. Values significantly different from that of the historical period at the 0.05 level (Student's t-test) are marked with larger and colored circles; otherwise they are in gray. All significant changes with days greater than one day are labeled. **c** Bars showing the proportion of the total number of weather whiplash in the historical period (the bar on the left) and in the long-term future (the bar on the right) with respect to their sum. An even split (i.e., 0.5) of the two bars indicates no change in the number of weather whiplash. The colors of the bars show the 30-year averaged multi-model weighted total number of weather whiplash in each period. The changes are shown for all stages in six East Asian land regions: (**1**) South China, (**2**) the mid-lower Yangtze River basin (MLYRB), (**3**) the Huai-Yellow River basin (HYRB), (**4**) North China, (**5**) South Japan and (**6**) the Korean Peninsula.

storage terms are trivial on the time scale of monsoon stages and are thereby omitted in Fig. 4.

Continental precipitation that scales at a slower rate than the C-C scaling[9,11,19,20,25,26,28] is tied to the tug of war between the

enhanced moisture effects and attenuated horizontal advection, vertical transport and convergence processes, especially during the warm-season stages (Fig. 3a–d(5)). Interestingly, the moisture effects along different dimensions exert markedly diverse impacts
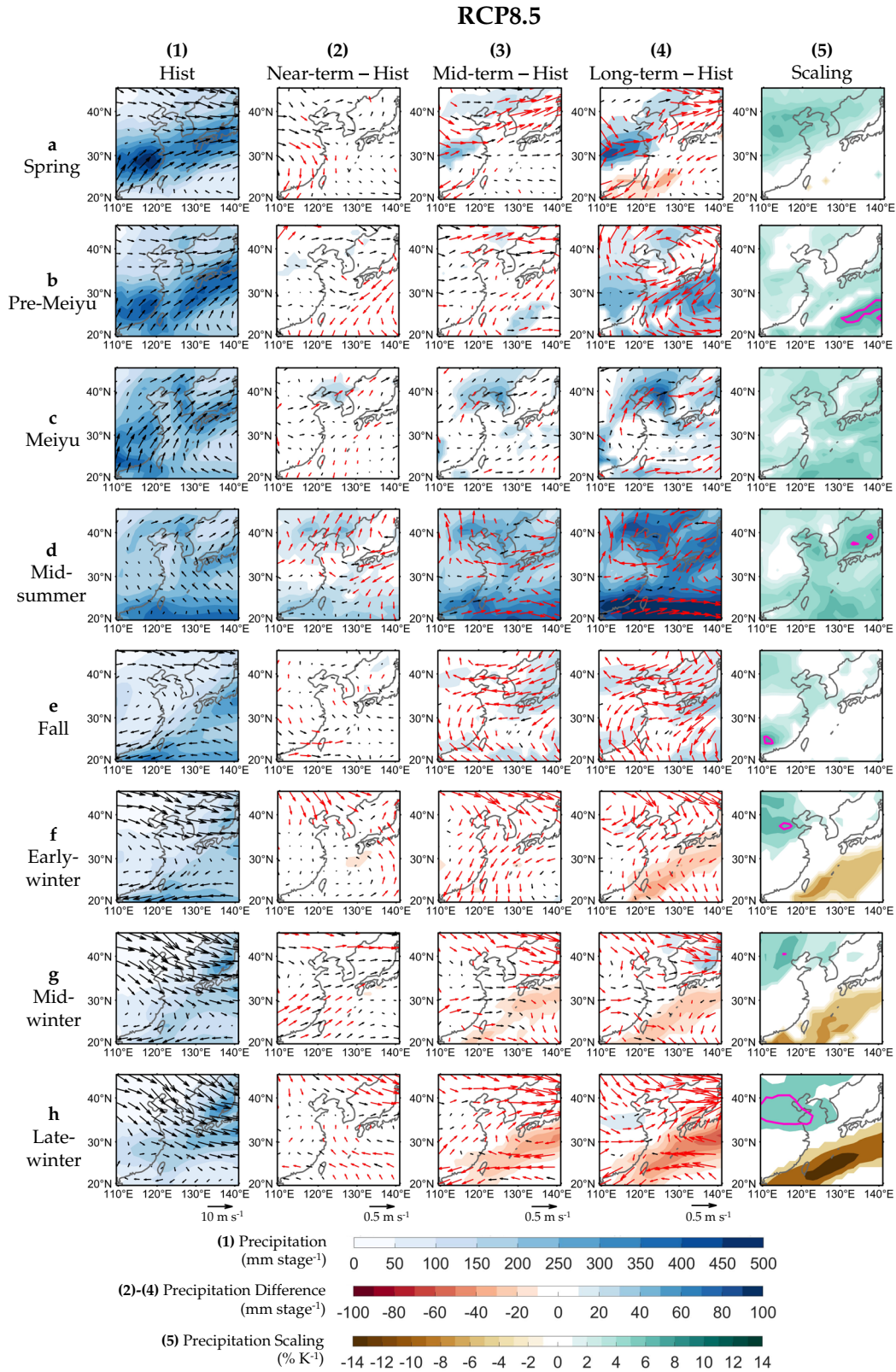
Fig. 3 Projected changes in monsoon patterns and precipitation scaling over East Asia. The multi-model weighted stage-mean precipitation (shading, unit: mm stage^{-1}) and 850-hPa winds (vector, unit: m s^{-1}) in (**1**) the historical period (1971–2100), and their differences with that in (**2**) the near-term (2011–2040), (**3**) mid-term (2041–2070) and (**4**) long-term future (2071–2100) from **a**–**h** the Spring to the Late-winter under the RCP8.5 scenario. (**5**) The fractional change of precipitation per degree of warming (i.e., precipitation scaling, unit: % K^{-1}) in each monsoon stage. The magenta contour denotes the estimated Clausius-Clapeyron scaling of 7% K^{-1}. All values shown in (**2**)–(**4**) are significant at the 0.05 level (Student's *t*-test).
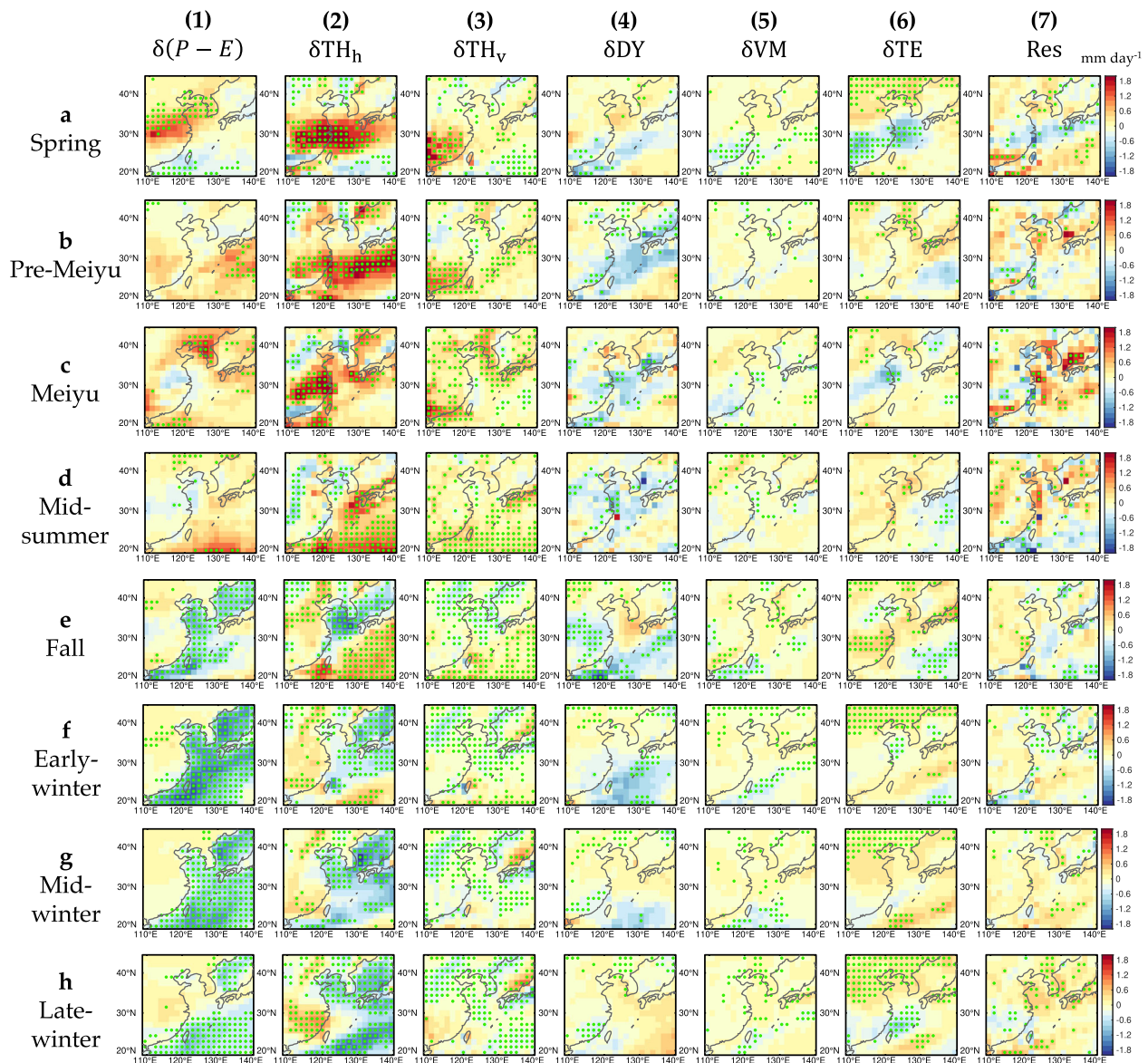
Fig. 4 Projected changes in atmospheric moisture budget during each monsoon stage. The changes in (**1**) the multi-model weighted stage-mean precipitation minus evaporation term $\delta(P–E)$, (**2**) the horizontal moisture-driven thermodynamic term (δTH_h), (**3**) the vertical thermodynamic term (δTH_v), (**4**) the dynamic term (δDY), (**5**) the vertical motion term (δVM), (**6**) the transient eddy moisture flux convergence term (δTE), and (**7**) the residuals (Res) from **a**–**h** the Spring to the Late-winter in the long-term future (2071–2100) compared to the historical period (1971–2000) under the RCP8.5 scenario. All values are in the unit of mm day^{-1}. Green stippling denotes the statistically significant values at the 0.05 level from the models (Student's t-test).

on the hydroclimate. For example, the horizontal moisture effect (δTH_h) explains most of the positive $\delta(P–E)$ in the MLYRB from the Spring to the Meiyu seasons, suggesting strengthened horizontal moisture transports for frontogenesis (Fig. 4a–c(1)–(3)). The vertical moisture effect (δTH_v), instead, accounts for enhanced precipitation exclusively along the southern coasts and over the Korean Peninsula, implying the role of enhanced moistening of the lower-troposphere in deep convections in the areas. As hinted earlier, the negative δDY, δVM and δTE components supported by a statistically significant model agreement, considerably offset the moisture effects in South China and the MLYRB (Fig. 4a–c(4)–(6)). These effects are commensurate with the weakened south-westerly monsoons and moisture flux convergence in the above

regions (Fig. 3a–c(4)). Notably, the negative δVM entails the tendency of descending motions that suppress the convection, which could result from the top-heavy heating effect[23,30] wherein a warmer upper troposphere leads to an increased atmospheric static stability in response to radiative forcings. In the dry season, δTH_h and δTE are projected to be the main contributors to the enhanced precipitation in the north (Fig. 4f–h(2), (6)), justifying the reduced wintertime drought risks as mentioned earlier (Fig. 2b).

Again, we report similar patterns of moisture budget components under the mitigated scenario (Supplementary Fig. 5), suggesting the robustness of the competing effects in both emission scenarios. However, it should be noted that CESM-CAM and inmcm4 models were both omitted in our moisture budget

analysis due to data scarcity, which unfortunately affects the moisture budget terms particularly for the Mid-summer stage where we saw a good performance by CESM-CAM. Given only a handful of grid cells with discernible residuals (Fig. 4a–h(7); see 'Methods' for discussion on uncertainties), we demonstrate the usefulness of the moisture budget analysis in attributing the causes of changing precipitation in the future EAM cycle.

A 'dry-get-wetter' paradigm in East Asia

The 'rich-get-richer' pattern is likely inapplicable to East Asia land regions; instead, we find evidence of a 'dry-get-wetter' paradigm in East Asia where the historically dry regions will become wetter, which are most evident in the rainy stages. Owing to the intraseasonal migration of monsoon rainbands during the warm season[1,2,38], monsoon onset and break periods often occur alternately across regions. During the Spring season, a positive precipitation scaling is expected in the north where the spring-time climate used to be relatively dry (Fig. 3a(1), (5)). Likewise, a wetter condition appears in the northern MLYRB where it was historically dry during the Pre-Meiyu stage (Fig. 3b(1), (5)). Similar 'dry-get-wetter' paradigms are discernible in places like the HYRB and North China during the Meiyu and winter stages (Fig. 3c, f–h). Recalling the projected moisture budget components, the weakening of monsoon circulations (i.e., negative δDY and δVM) and transient eddies of moisture flux divergence (i.e., a negative δTE) explains the 'wet-not-get-wetter' paradigm in the historically wet regions (e.g., Fig. 4a–c). Conversely, horizontal and vertical moisture effects (i.e., positive δTH_h and δTH_v) are the primary causes of the 'dry-get-wetter' paradigm found over land during several intraseasonal stages. Unawareness of such a 'dry-get-wetter' paradigm might miss the golden timings of agricultural production and flood adaptations under climate change, potentially putting societal security at risk.

In contrast, the marine climate over the western North Pacific presents a 'rich-get-richer' paradigm[20,39,40] across monsoon stages under greenhouse warming. A 'wet-get-wetter' pattern is evident over oceans from the Pre-Meiyu to the Mid-summer (Fig. 3b–d) mainly due to the horizontal moistening effect (δTH_h) (Fig. 4b–d). In wintertime, we notice a sudden sign switch of δTH_h (i.e., a horizontal drying effect) coupled with weakened monsoon circulations (i.e., a negative δDY), giving rise to an overall 'dry-get-drier' pattern over the oceans (Figs. 3f–h, 4f–h).

DISCUSSION

The present study contributes to an improved understanding of the projected changes in the intraseasonal monsoon stages that have once been a missing piece in the EAM research. In the following, we summarize several robust and systematic changes in a warming EAM climate and discuss the societal implications and the possible mechanisms at work.

In terms of monsoon seasonality, we unveil a skewed EAM annual cycle manifest in a prolonged rainy season at the cost of delayed, shortened, and weakened winter stages, which is most evident in the late-21st century under the high-end scenario. Such a lengthened rainy season originates from the extension of the Mid-summer and the Fall stages, inferring a longer transition from the warm to the cold season than the reverse way. While a stretched rainy season may favor sowing and harvesting, it also accompanies a greater and earlier flood risk in the entire East Asian continent, with alarmingly 14–20 more heavy precipitation days on average throughout the warm season in the worst-case scenario. However, future hydrological risks would be significantly reduced given substantial mitigations to reduce carbon emissions as soon as possible. Forward-looking adaptations are also required to cope with the soaring flood potential, especially during the Spring and the Mid-summer. We pay special attention to the

MLYRB where floods are projected to come earlier with more severe impacts, given the enhanced springtime rainfall compounded with the upstream snow melting and the potential outburst of the ice-dammed glacial lakes[34]. Apart from a continent-wide increase of precipitation, the Mid-summer flood risk will be heightened by the antecedent wetness of the soil due to the previous rainy stages, causing entire East Asia to be more prone to floods. The projected rise of drought risks when transitioning to the prolonged Fall and the delayed Early-winter could potentially disrupt harvesting, wintertime water security, and ecosystem services. More snowfall or cold rains may occur in the HYRB, North China, and the Korean Peninsula despite a shortened winter. Notably, more frequent weather whiplash is expected in East Asia, especially over the HYRB, South Japan and the Korean Peninsula during the stages outside the peak summer and winter seasons, which could cause more severe societal impacts than weather extremes individually.

We present evidence of the rarely-documented 'dry-get-wetter' paradigm in East Asia, demonstrating the complexity of a subtropical monsoon system like the EAM, in which the commonly believed 'rich-get-richer' mechanism[39,40] could not universally apply to the region[24]. The complete moisture budget decomposition unravels the role of the horizontal and vertical moisture effects (δTH_h and δTH_v) in the 'dry-get-wetter' regions during the warm-season stages, while the weakening of the dynamic effect (δDY), transient eddies of moisture convergence (δTE) and the vertical motions (δVM) elucidate the 'wet-not-get-wetter' paradigm in the historically wet regions. Broadly in tune with the previous studies[9,11,19,20,28], we further show that the competition between the enhanced moisture effects (both horizontally and vertically) and the attenuated horizontal advection, vertical motions and convergence explains slower precipitation scaling than the C-C relation, as evident in the warm-season stages.

One possible mechanism for the skewed monsoon cycle could link with the change of the westerly jet stream. During the prolonged Mid-summer in a warmer climate, we observe a stronger westerly jet lingered on the southern Tibetan Plateau due to an enhanced meridional temperature gradient in the mid-troposphere by the thermal wind relation (Supplementary Fig. 6d). The intensified jet stream in the south could facilitate the frontogenesis and convective initiations in East Asia[41,42], and may thereby sustain the Mid-summer monsoon circulations (Fig. 3d(1)). In contrast, faster surface warming near 40˚N, as evident in the Mid-summer and the Fall, attenuates the westerlies and induces a cyclonic circulation anomaly at the upper level (Supplementary Fig. 6d, e). This atmospheric response may suppress the development of the wintertime Siberian high and partly explain the postponement of the winter stages (Fig. 1a, c). The cause of the weakened Asian monsoon circulations, as revealed from the moisture budget decomposition, could stem from the enhanced condensational heating in the upper troposphere in the tropics[9,13], which consequently weakens the planetary-scale meridional thermal gradient and thereby the monsoon circulations[43,44]. The physical processes triggering the skewed monsoon cycle and the weakened monsoon circulations warrant further verification.

It should be noted that the multi-model weighting scheme proposed in this study provides a technical alternative to investigate the projected monsoon climate. It may be improved by considering further the mutual independence among the models[45]. While the systematic biases in the models may be reduced by the multi-model scheme and temporal differences in climate periods, the extent to which the biases impact the results, on both the mean state and the intraseasonal variability, is worth in-depth investigation.

Findings from this work provide policymakers, farmers, water managers and other stakeholders in East Asia, with practical information about the projected changes of the intraseasonal

monsoon stages that are more pertinent to agricultural activities, climate policies and adaptations, land-use planning and water management. This study lays the foundation of our future work on the intraseasonal EAM climate under the Shared Socioeconomic Pathways (SSP) scenarios by the next generation of climate models.

METHODS

Data

The fifth generation European Centre for Medium-Range Weather Forecast (ECMWF) atmospheric reanalysis (ERA5) at 1.5° gird resolution during 1979–2005 is adopted as a benchmark dataset to validate climate models' performance. We analyze outputs from 13 medium-to-high spatial resolutions climate models from CMIP5[46] (Supplementary Table 1) for their greater potentials in reproducing the EAM climate than the coarser-resolution models[47]. Model outputs are retrieved from the historical run in 1971–2005 and the RCP4.5 and 8.5 scenarios in 2006–2100. We also include outputs from a 40-member ensemble of fully-coupled Community Earth System Model version 1 (CESM1) with the National Center of Atmospheric Research (NCAR) Community Atmosphere Model (CAM 5.2) being its atmospheric component (hereafter termed as the CESM-CAM5 model)[48], which performs the RCP8.5 projection as the CMIP5 models. The multi-ensembles mean for each model is computed for further analysis. As the spatial resolution is different across models, all the model output fields are linearly interpolated into 1.5° gird resolution for a direct comparison to the benchmark fields.

Derivation of EAM annual cycle and the related definitions

We follow the approach developed by Dai et al. (2021)[17] to construct the EAM annual cycle, which employs a 1×8 Self-organizing Map (SOM)[49] to derive eight distinct monsoon stages in the EAM domain (109.5–141°E, 19.5–45°N) based on the daily climatology of 850-hPa horizontal winds smoothed by the 5-day-moving-mean. The clustering is trained with 850-hPa winds in the historical run (1979–2005) in each climate model, and the results are then evaluated against that from the training with the ERA5 reanalysis. Readers are referred to Dai et al.[17] for more details of the approach.

The stage onset date is defined as the starting day of the first five consecutive days of the corresponding stage in the year after the stage assignment[17]. Likewise, the retreat date is the last day of the last five consecutive days of the corresponding stage. Given the purely data-driven definitions, a stage's retreat date could sometimes occur later than the onset date of the ensuing stage. To avoid double-counting the days in our analysis, we investigate the number of days of a stage in one annual cycle so as to infer its duration. The 5-day persistence is defined as the conditional probability that if the first day belongs to a stage, the ensuing four days belong to the same stage. The change of the metric infers whether the stage becomes more persistent or intermittent.

Multi-model weighting scheme

Three indices considering the temporal and spatial features of the monsoon stages are designed to filter the well-performed models in reproducing the EAM annual cycle. For each monsoon stage, we compute two ratios of the time overlapped to either the observed or the model's stage period (O_1 and O_2) to evaluate the overall temporal matching, namely,

$$O_1 = (T_o \cap T_m)/T_o, \tag{1}$$

$$O_2 = (T_o \cap T_m)/T_m, \tag{2}$$

where T_o and T_m is a set of calendar days of the observed and model's stage period, respectively, and $\cap$ denotes the intersection. The third index is the spatial pattern correlation coefficient R to evaluate the spatial similarity of the climatological 850-hPa wind fields in the corresponding observed stage and that in the model simulation. For each monsoon stage, we then select well-performed models given all three indices (i.e., O_1, O_2, and R) greater than 0.5. The rationale of this preprocessing is to remove poorly performed models that could undermine the confidence of the analysis. Detailed results of the model selection are listed in Supplementary Table 2.

Here, we propose a weighting scheme in terms of the model's potential in simulating the temporal and spatial features of the monsoon stage (Supplementary Fig. 7a). Specifically, for each monsoon stage, the

weighting w_i assigned to a selected model i is defined as

$$w_i = \frac{\left[(1 - O_{2,i})^2 + D_i^2\right]^{-\frac{1}{2}}}{\sum_i^n \left[(1 - O_{2,i})^2 + D_i^2\right]^{-\frac{1}{2}}}, \tag{3}$$

where D_i denotes the Euclidean distance in climatological 850-hPa wind fields between the observed stage and the simulated stage from model i, and n denotes the number of selected models for the monsoon stage. Note that we scaled D_i from 0 to 1 to make it comparable to O_2 prior to the calculation of weightings. Only O_2 is considered in Eq. (3) as it is directly proportional to O_1 (Eqs. (1) and (2)). Results using the weighting scheme largely outperform individual models based on the stages' temporal characteristics (i.e., onset, retreat and number of days), the 850-hPa winds, precipitation and temperature patterns (Supplementary Fig. 7b–h). Albeit with a comparable performance of the multi-model weighting and the arithmetic averaging schemes, the weighting scheme is still adopted for analysis as it is based on more reliable models (Supplementary Fig. 7b, f).

Hydrological risk analysis

For each East Asian land region, dry days (heavy precipitation days) are obtained by the number of days with the regional-total precipitation lower (higher) than the 10th (90th) percentile of the historical values (1971–2000) during each monsoon stage for each climate model. We compute the likelihood by dividing the dry or heavy precipitation days by the number of days of a stage. Regarding the weather whiplash (i.e., an abrupt shift between two opposite weather extremes), it is defined as a dry day and a heavy precipitation day that occur one after another within five days. The total number of weather whiplash in a monsoon stage is determined by the period between its onset date and that of the ensuing stage. The multi-model weighting scheme is applied to the likelihood of heavy precipitation days, dry days, and the frequency of occurrence of weather whiplash deduced from each model (Fig. 2).

Moisture budget decomposition

To evaluate the extent to which the changes in different processes (e.g., thermodynamic, dynamic, and transient effects) would contribute to the change of precipitation, we start from the vertically integrated atmospheric moisture budget equation[50], which writes

$$P - E = -\frac{\partial w}{\partial t} - \frac{1}{\rho_w g} \nabla \cdot \int_0^{p_s} q\mathbf{u} \, dp, \tag{4}$$

where P is the precipitation, E is the evaporation, w is the precipitable water in the atmosphere, ρ_w is the density of water, g is the gravitational acceleration, q is the specific humidity, $\mathbf{u}$ is the three-dimensional wind consisting of horizontal wind velocities and pressure velocity ω, and p_s denotes surface pressure. Inspired by Seager et al.[51]'s derivation, the changes in the moisture budget between two time periods can be written in a complete form:

$$\delta(P - E) = \delta\text{TH}_h + \delta\text{TH}_v + \delta\text{DY} + \delta\text{VM} + \delta\text{TE} + \delta\text{NL} + \delta\text{ST} + \text{Res}, \tag{5}$$

$$\text{where } \delta\text{TH}_h = -\frac{1}{\rho_w g} \int_{10\,\text{hPa}}^{1000\,\text{hPa}} \nabla_h \cdot (\overline{\mathbf{u}}_{his}\delta\overline{q}) dp, \tag{6}$$

$$\delta\text{TH}_v = -\frac{1}{\rho_w g} \int_{10\,\text{hPa}}^{1000\,\text{hPa}} \frac{\partial}{\partial p} (\overline{\omega}_{his}\delta\overline{q}) dp, \tag{7}$$

$$\delta\text{DY} = -\frac{1}{\rho_w g} \int_{10\,\text{hPa}}^{1000\,\text{hPa}} \nabla_h \cdot (\overline{q}_{his}\delta\overline{\mathbf{u}}) dp, \tag{8}$$

$$\delta\text{VM} = -\frac{1}{\rho_w g} \int_{10\,\text{hPa}}^{1000\,\text{hPa}} \frac{\partial}{\partial p} (\overline{q}_{his}\delta\overline{\omega}) dp, \tag{9}$$

$$\delta\text{TE} = -\frac{1}{\rho_w g} \int_{10\,\text{hPa}}^{1000\,\text{hPa}} \nabla \cdot \delta(\overline{q'\mathbf{u}'}) dp, \tag{10}$$

$$\delta\text{NL} = -\frac{1}{\rho_w g} \int_{10\,\text{hPa}}^{1000\,\text{hPa}} \nabla \cdot (\delta\overline{\mathbf{u}}\delta\overline{q}) dp, \tag{11}$$

$$\delta\text{ST} = -\frac{1}{\rho_w g} \int_{10\,\text{hPa}}^{1000\,\text{hPa}} \delta\left(\frac{\overline{\partial q}}{\partial t}\right) dp, \tag{12}$$

and

$$\delta(\cdot) = (\cdot)_{fut} - (\cdot)_{his}. \tag{13}$$

In this context, overbars indicate the climatological stage-means and primes are the departures from the climatological stage-means. $\delta(\cdot)$ denotes the difference in the quantity between the future and historical periods. ∇ and ∇_h indicate the three-dimensional and horizontal divergence operators, respectively. $\delta(P–E)$ refers to the change in the net flux of water substance at the surface. δTH_h and δTH_v represents the moisture-driven thermodynamic effect in response to the change in the horizontal and vertical gradients of specific humidity, respectively. δDY is the horizontal dynamic effect, while δVM is the vertical motion term that could be induced by both mechanical and thermal forcings. δTE represents the change in transient eddies of moisture flux convergence, δNL is the nonlinear term, and δST is the water storage term. Since the vertical integration is merely computed from 10 to 1000 hPa, here we preserve the vertical component (i.e., δTH_v and δVM) to explain the precipitation change in the convective region[27,39,52]. Note that the pressure-level data underneath the topography were removed from the vertical integral. We omitted the CESM-CAM5 and inmcm4 models in the moisture budget analysis due to data scarcity. For the same token, the surface term in the original derivation[51] was incorporated into the residual term (Res). Large residuals could be found in regions with complex topography (e.g., in mountainous or coastal areas) (Fig. 4), where data with a coarse vertical resolution fail to represent the state of the system[29,50]. As daily evaporation is not available in the CMIP5 model outputs, we assume all days of the month share the same rate of evaporation bounded by the monthly amount. All the terms were first computed for each model and were then interpolated to a common $1.5˚ \times 1.5˚$ gridded resolution before performing the multi-model weighted averaging.

Statistical significance

We adopted a two-tailed Student's t-test with a significance level of 0.05 in all analyses present in this article. The t-test was performed with the null hypothesis that annual values of a given 30-year period come from a t-distribution with a mean equal to the historical mean (e.g., Figs. 1–3) with an unknown variance. For Fig. 4, the t-test was conducted on the time-mean of a given period from the climate models with the null hypothesis that the mean is zero and variance is unknown.

DATA AVAILABILITY

The meteorological data is retrieved from the ERA5 by the European Center for Medium-Range Weather Forecast (ECMWF) at https://www.ecmwf.int/en/forecasts/datasets/reanalysis-datasets/era5. The CMIP5 data can be accessed from https://esgf-node.llnl.gov/search/cmip5/. CESM-CAM5 outputs from the CESM Large Ensemble Community Project is available from https://www.cesm.ucar.edu/projects/community-projects/LENS/data-sets.html. Derived data supporting the findings of this study are available from the corresponding author upon reasonable request.

CODE AVAILABILITY

The source codes for the analysis of this study are available from the corresponding author upon reasonable request.

REFERENCES

1. Ding, Y. & Chan, J. C. L. The East Asian summer monsoon: an overview. *Meteorol. Atmos. Phys.* **89**, 117–142 (2005).
2. Wang, B. & Lin, H. O. Rainy season of the Asian-Pacific summer monsoon. *J. Clim.* **15**, 386–398 (2002).
3. Son, J. H., Seo, K. H. & Wang, B. Dynamical control of the Tibetan Plateau on the East Asian summer monsoon. *Geophys. Res. Lett.* **46**, 7672–7679 (2019).
4. Chiang, J. C. H. et al. Role of seasonal transitions and westerly jets in East Asian paleoclimate. *Quat. Sci. Rev.* **108**, 111–129 (2015).
5. Wang, B. *The Asian Monsoon*. (Springer, 2006).
6. Li, C. & Yanai, M. The Onset and interannual variability of the Asian Summer Monsoon in relation to Land–Sea thermal contrast. *J. Clim.* **9**, 358–375 (1996).
7. Dong, G. et al. CMIP5 model-simulated onset, duration and intensity of the Asian summer monsoon in current and future climate. *Clim. Dyn.* **46**, 355–382 (2016).
8. Zhang, H., Liang, P., Moise, A. & Hanson, L. Diagnosing potential changes in Asian summer monsoon onset and duration in IPCC AR4 model simulations using moisture and wind indices. *Clim. Dyn.* **39**, 2465–2486 (2012).
9. Ueda, H., Iwai, A., Kuwako, K. & Hori, M. E. Impact of anthropogenic forcing on the Asian summer monsoon as simulated by eight GCMs. *Geophys. Res. Lett.* **33**, 20–23 (2006).
10. Kitoh, A. & Uchiyama, T. Changes in onset and withdrawal of the East Asian summer rainy season by multi-model global warming experiments. *J. Meteorol. Soc. Jpn.* **84**, 247–258 (2006).
11. Christensen, J. H. et al. Climate Phenomena and ther Relevance for Future Regional Climate Change. (Chapter 14 in *Climate Change 2013 The Physical Science Basis Working Group I Contribution to the Fifth Assessment Report of the Intergovernmental Panel on Climate Change*, 1217–1310 (Cambridge University Press, 2013).
12. Ha, K. J., Moon, S., Timmermann, A. & Kim, D. Future changes of summer monsoon characteristics and evaporative demand over Asia in CMIP6 simulations. *Geophys. Res. Lett.* **47**, 1–10 (2020).
13. Kitoh, A. et al. Monsoons in a changing world: a regional perspective in a global context. *J. Geophys. Res. Atmos.* **118**, 3053–3065 (2013).
14. Lee, J.-Y. & Wang, B. Future change of global monsoon in the CMIP5. *Clim. Dyn.* **42**, 101–119 (2014).
15. Wang, J. et al. Changing lengths of the four seasons by global warming. *Geophys. Res. Lett.* **48**, 1–9 (2021).
16. Ding, Y. in *East Asian Monsoon* (ed. Chang, C.-P.) 3–53 (World Scientific Publishing Co., 2004).
17. Dai, L., Cheng, T. F. & Lu, M. Define East Asian monsoon annual cycle via a self-organizing map-based approach. *Geophys. Res. Lett.* **48**, e2020GL089542 (2021).
18. Sah, R. K. Tropical Economies and Weather Information. in *Monsoons* (eds. Fein, J. S. & Stephens, P. L.) 105–120 (John Wiley & Sons, Inc., 1987).
19. Moon, S. & Ha, K. J. Future changes in monsoon duration and precipitation using CMIP6. *npj Clim. Atmos. Sci.* **3**, 1–7 (2020).
20. Held, I. M. & Soden, B. J. Robust responses of the hydrological cycle to global warming. *J. Clim.* **19**, 5686–5699 (2006).
21. Li, Z., Sun, Y., Li, T., Ding, Y. & Hu, T. Future changes in East Asian summer monsoon circulation and precipitation under 1.5 to 5 °C of warming. *Earth's Future* **7**, 1391–1406 (2019).
22. Hsu, P. C. et al. Increase of global monsoon area and precipitation under global warming: a robust signal? *Geophys. Res. Lett.* **39**, 2–7 (2012).
23. Wang, B., Jin, C. & Liu, J. Understanding future change of global monsoons projected by CMIP6 models. *J. Clim.* **33**, 6471–6489 (2020).
24. Chadwick, R., Boutle, I. & Martin, G. Spatial patterns of precipitation change in CMIP5: why the rich do not get richer in the tropics. *J. Clim.* **26**, 3803–3822 (2013).
25. O'Gorman, P. A. & Muller, C. J. How closely do changes in surface and column water vapor follow Clausius-Clapeyron scaling in climate change simulations? *Environ. Res. Lett.* **5**, 025207 (2010).
26. Trenberth, K. E., Dai, A., Rasmussen, R. M. & Parsons, D. B. The changing character of precipitation. *Bull. Am. Meteorol. Soc.* **84**, 1205–1217 (2003).
27. Jin, C., Wang, B. & Liu, J. Future changes and controlling factors of the eight regional monsoons projected by cmip6 models. *J. Clim.* **33**, 9307–9326 (2020).
28. Tanaka, H. L., Ishizaki, N. & Nohara, D. Intercomparison of the Intensities and Trends of Hadley, Walker and Monsoon Circulations in the Global Warming Projections. *Sola* **1**, 77–80 (2005).
29. Endo, H. & Kitoh, A. Thermodynamic and dynamic effects on regional monsoon rainfall changes in a warmer climate. *Geophys. Res. Lett.* **41**, 1704–1710 (2014).
30. Wang, B., Yim, S. Y., Lee, J. Y., Liu, J. & Ha, K. J. Future change of Asian-Australian monsoon under RCP 4.5 anthropogenic warming scenario. *Clim. Dyn.* **42**, 83–100 (2014).
31. Ma, J., Xie, S. P. & Kosaka, Y. Mechanisms for tropical tropospheric circulation change in response to global warming. *J. Clim.* **25**, 2979–2994 (2012).
32. Sun, Y. & Ding, Y. A projection of future changes in summer precipitation and monsoon in East Asia. *Sci. China Earth Sci.* **53**, 284–300 (2010).
33. Thackeray, C. W. & Fletcher, C. G. Snow albedo feedback: Current knowledge, importance, outstanding issues and future directions. *Prog. Phys. Geogr.* **40**, 392–408 (2016).
34. Zheng, G. et al. Increasing risk of glacial lake outburst floods from future Third Pole deglaciation. *Nat. Clim. Chang.* **11**, 411–417 (2021).
35. Chiang, J. C. H., Swenson, L. M. & Kong, W. Role of seasonal transitions and the westerlies in the interannual variability of the East Asian summer monsoon precipitation. *Geophys. Res. Lett.* **44**, 3788–3795 (2017).
36. Wang, S. S. Y. et al. Consecutive extreme flooding and heat wave in Japan: are they becoming a norm? *Atmos. Sci. Lett.* **20**, 2–5 (2019).
37. Lu, Y., Hu, H., Li, C. & Tian, F. Increasing compound events of extreme hot and dry days during growing seasons of wheat and maize in China. *Sci. Rep.* **8**, 1–8 (2018).

38. Dai, L., Cheng, T. F. & Lu, M. Summer monsoon rainfall patterns and predictability over Southeast China. *Water Resour. Res.* **56**, 1–21 (2020).

39. Chou, C., Neelin, J. D., Chen, C. A. & Tu, J. Y. Evaluating the 'rich-get-richer' mechanism in tropical precipitation change under global warming. *J. Clim.* **22**, 1982–2005 (2009).

40. Trenberth, K. E. Changes in precipitation with climate change. *Clim. Res* **47**, 123–138 (2011).

41. Yuan, Z., Zhuge, X. & Wang, Y. The forced secondary circulation of the Mei-yu Front. *Adv. Atmos. Sci.* **37**, 766–780 (2020).

42. Chiang, J. C. H., Fischer, J., Kong, W. & Herman, M. J. Intensification of the Pre-Meiyu Rainband in the Late 21st Century. *Geophys. Res. Lett.* **46**, 7536–7545 (2019).

43. Sooraj, K. P., Terray, P. & Mujumdar, M. Global warming and the weakening of the Asian summer monsoon circulation: assessments from the CMIP5 models. *Clim. Dyn.* **45**, 233–252 (2015).

44. Dai, A. et al. The relative roles of upper and lower tropospheric thermal contrasts and tropical influences in driving Asian summer monsoons. *J. Geophys. Res. Atmos.* **118**, 7024–7045 (2013).

45. Wang, B. et al. Advance and prospectus of seasonal prediction: assessment of the APCC/ CliPAS 14-model ensemble retrospective seasonal prediction (1980–2004). *Clim. Dyn.* **33**, 93–117 (2009).

46. Taylor, K. E., Stouffer, R. J. & Meehl, G. A. An overview of CMIP5 and the experiment design. *Bull. Am. Meteorol. Soc.* **93**, 485–498 (2012).

47. Kim, H. J., Wang, B. & Ding, Q. The global monsoon variability simulated by CMIP3 coupled climate models. *J. Clim.* **21**, 5271–5294 (2008).

48. Kay, J. E. et al. The community earth system model (CESM) large ensemble project: a community resource for studying climate change in the presence of internal climate variability. *Bull. Am. Meteorol. Soc.* **96**, 1333–1349 (2015).

49. Kohonen, T. The self-organizing map. *Neurocomputing* **21**, 1–6 (1998).

50. Trenberth, K. E. & Guillemot, C. J. Evaluation of the global atmospheric moisture budget as seen from analyses. *J. Clim.* **8**, 2255–2272 (1995).

51. Seager, R., Naik, N. & Vecchi, G. A. Thermodynamic and dynamic mechanisms for large-scale changes in the hydrological cycle in response to global warming. *J. Clim.* **23**, 4651–4668 (2010).

52. Zhou, S., Huang, G. & Huang, P. Changes in the East Asian summer monsoon rainfall under global warming: moisture budget decompositions and the sources of uncertainty. *Clim. Dyn.* **51**, 1363–1373 (2018).

53. Wehrens, R. & Buydens, L. M. C. Self- and super-organizing maps in R: the kohonen package. *J. Stat. Softw.* **21**, 1–19 (2007).

AUTHOR CONTRIBUTIONS

M.L. conceived and supervised the study. L.D. conducted the analyses of projected intraseasonal timings, hydrological risks and meteorological patterns in future monsoon stages. T.F.C. prepared the climate model data, performed the moisture budget analysis and contributed the diagnostic discussion. All co-authors contributed to the discussion of results, and the writing and revision of the manuscript.

COMPETING INTERESTS

The authors declare no competing interests.

ADDITIONAL INFORMATION

Supplementary information The online version contains supplementary material available at https://doi.org/10.1038/s41612-022-00235-9.

Correspondence and requests for materials should be addressed to Mengqian Lu.

Reprints and permission information is available at http://www.nature.com/reprints

Publisher's note Springer Nature remains neutral with regard to jurisdictional claims in published maps and institutional affiliations.